EPJ Web of Conferences **25**, 01037 (2012)
DOI: 10.1051/epjconf/20122501037

EXPERIMENTAL INVESTIGATION OF THE EFFECT OF LIQUID VISCOSITY ON SLUG FLOW IN SMALL DIAMETER BUBBLE COLUMN

Olumayowa Timothy KAJERO, Barry John AZZOPARDI, Lokman ABDULKAREEM

Abstract

The effect of liquid viscosity on slug flow in a 50 mm diameter bubble column was investigated experimentally using air-silicone oil as operating fluid with silicone oil of viscosities 5, 100, 1000 and 5000 mPa.s. Data was collected using Electrical Capacitance Tomography (ECT), a non-intrusive advanced instrumentation measuring technique and the high Speed Video Camera, through which the slug parameters such as length of Taylor bubbles and liquid slug, void fraction in Taylor bubbles and liquid slug, slug frequency, film thickness and pressure gradient in the slug, were measured and analyzed. The analysis was done using the void fraction time series, probability density function and power spectral density plots. Superficial gas velocities of $0.02 \leq U_{gs} \leq 0.361$ m/s were used in the experiment. It was also observed that as viscosity increases, slug frequency, structure velocity, length of liquid slug, void fraction in liquid slug and void fraction in Taylor bubbles decreases; while the length of Taylor bubble, film thickness and pressure gradient in the slug increases.

Keywords: *ECT, Slug, Void fraction, Taylor bubble, Pressure gradient*

INTRODUCTION

Slug flow is encountered in the heat and mass transfer between gas and liquid in chemical reactors, most especially when it involves highly viscous liquid in either small or large diameter bubble columns. The use of highly viscous liquid in small diameter bubble columns results in slug flow which involves the appearance of typically bullet-shaped large pockets of gas called Taylor bubbles which occupy a large part of the cross-section of the column. The knowledge of the effect of physical properties of liquid is a key factor in the study of the behaviour of gas-liquid flow. The property of concern here is liquid viscosity. Variation in viscosity influences the slug flow characteristics. Several investigators have carried out different studies on slug, however few studies were found on the effect of liquid viscosity on slug flow.

Olumayowa Timothy KAJERO[1], Barry John AZZOPARDI[2], Lokman ABDULKAREEM[3]

Process and Environmental Engineering Research Division, Faculty of Engineering, University of Nottingham, University Park, NG7 2RD, United Kingdom,
[1]enxotk@nottingham.ac.uk, [2]barry.azzopardi@nottingham.ac.uk, [3]ezala@nottingham.ac.uk

The use of small diameter columns constitutes the wall effect which occurs as a result of the impact of the wall of the column on the liquid [18]. The small diameter creates a constraint on the liquid causing it to take the shape of a bullet which is called Taylor bubbles. It has also been found that the void fraction in small diameter column was slightly higher than that in large diameter columns due to the wall effect [8], [30].

Wall effect hinders the bubble rise velocity when the ratio of bubble diameter to column diameter is greater than 0.125 which eventually leads to increase in void fraction [8], [28]. Hence, smaller wall effects are observed in larger diameter columns [16], [19], [20].

BACKGROUND TO THE STUDY

[6] and [29] investigated the effect of liquid viscosity on slug characteristics in near horizontal pipes. [24] experimentally studied the effect of liquid viscosity on liquid holdup in the slug unit, film region and slug zone in the aerated slug flow region using three fluid systems: air-light oil (μ =17 mPa.s), air-heavy oil (μ =17 mPa.s) and air-water systems. They observed that as viscosity increases, there was a significant increase of liquid holdup in the slug unit and film region, with less significant increase of liquid holdup in the slug zone. The film liquid holdup was said to be directly proportional to the liquid viscosity due to an increase in the interfacial and wall shear forces on the liquid film. [2] from the empirical correlation developed for slug liquid holdup as a function of liquid viscosity explained that the slug liquid holdup is directly proportional to the liquid viscosity [27] and [15] reported an increase in slug frequency with increasing liquid viscosity for which they developed an empirical slug flow correlation.

[1] studied the characteristics of slug flow in a vertical riser using the ECT. They used air-silicone oil as the model fluids over a range of gas and liquid superficial velocities of (0.344 - 0.745 m/s) and (0.047 - 0.38 m/s), respectively. The viscosity of silicone oil they used is 5 mPa.s, they found that the lengths of the liquid slug and Taylor bubbles increased with an increase in gas superficial velocity. They also observed that the void fraction in the liquid slug and Taylor bubbles also increased with an increase in gas superficial velocity. They concluded that the slug frequency increased with an increase in liquid superficial velocity and that the gas superficial velocity had a negligible effect on it.

Slug flow structure in bubble column

Slug flow can be described by a succession of identical unit cells each consisting of:

Taylor bubble: a cylindrical bubble, which are large pockets of gases bullet shaped in pattern. It has a front or nose which is spherical. The shape of the Taylor bubble according to [10] is dependent on whether or not viscous force is negligible. When negligible, this is referred to as the inertia controlled regime in which the bubble has a flat back, indicating flow separation occurs. In the film, gravity forces the liquid film to fall and it impinges the liquid slug causing flow separation at the bubble tail. The type of shape obtained in this case is called Prolate spheroid. It is obtained when the inverse dimensionless viscosity, N_f is greater than 300. When viscous effects are significant, the bubble tail or back is shaped like an oblate spheroid in which both the front and back of the Taylor bubble are curved. The viscous regime occurs when the inverse dimensionless viscosity, N_f is less than 2 [36] in which the pipe diameter is less than 1.6 $\left(\mu_L^2 \rho_L^{-2} g^{-1}\right)^{1/3}$ applicable to highly viscous liquids.

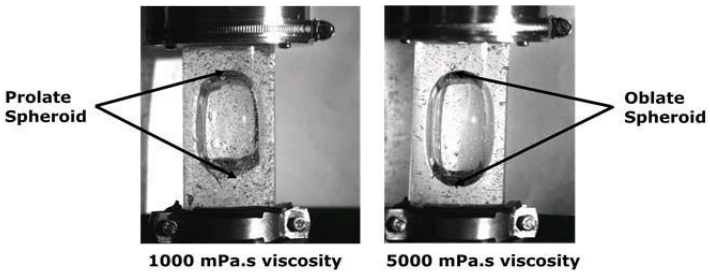

Figure 1: Prolate and Oblate Spheroid Taylor bubbles (taken using the high speed video camera)

Falling Liquid Film: These are thin film of liquid surrounding the Taylor bubble. The liquid film usually flows into subsequent liquid slug causing bubble entrainment in the liquid slug and also flow separation at the bubble tail [17]. The flow of the liquid into the liquid slug is due to the force of gravity.

Liquid Slug: These are dispersion of small bubbles below the Taylor bubble. The liquid slug has been described to be quite complex. Three distinct regions have been identified by [23]. They considered a pipe 26mm in diameter, using air/water at 2 bar and superficial gas velocities of 0.2 – 5m/s and superficial liquid velocity of 0.1 – 3m/s. [31] identified the region close to the Taylor bubble's tail as the liquid swelling zone or the swelling region front zone. It is the region where gas is being entrained from and returned to the Taylor bubble and is of 0.15 – 5 pipe diameter. Directly below this region, is the wake zone of about 1 – 10 pipe diameter long [17]. It is a cluster of bubbles which is said to contain the vortex according to [35]. There is a linear increase in the length of the liquid swelling and wake zone with increase in superficial gas velocity but with less effect with superficial liquid velocity. Next to the wake zone, is the low void fraction zone which extends down to the next Taylor bubble and is about 1 – 19 pipe diameter long. [4] combined the liquid swelling zone with the Taylor bubble, considering majorly the wake and low void fraction zones [3].

The slug flow structure is as shown in figure 2.

Where:

L_{TB} = Length of Taylor bubble, m

L_{LS} = Length of Liquid Slug, m

L_{SU} = Length of Slug unit, m

ε_{TB} = Void fraction of the Taylor bubble

ε_{LS} = Void fraction of the liquid slug

U_{TB} = Velocity of Taylor bubble, m/s

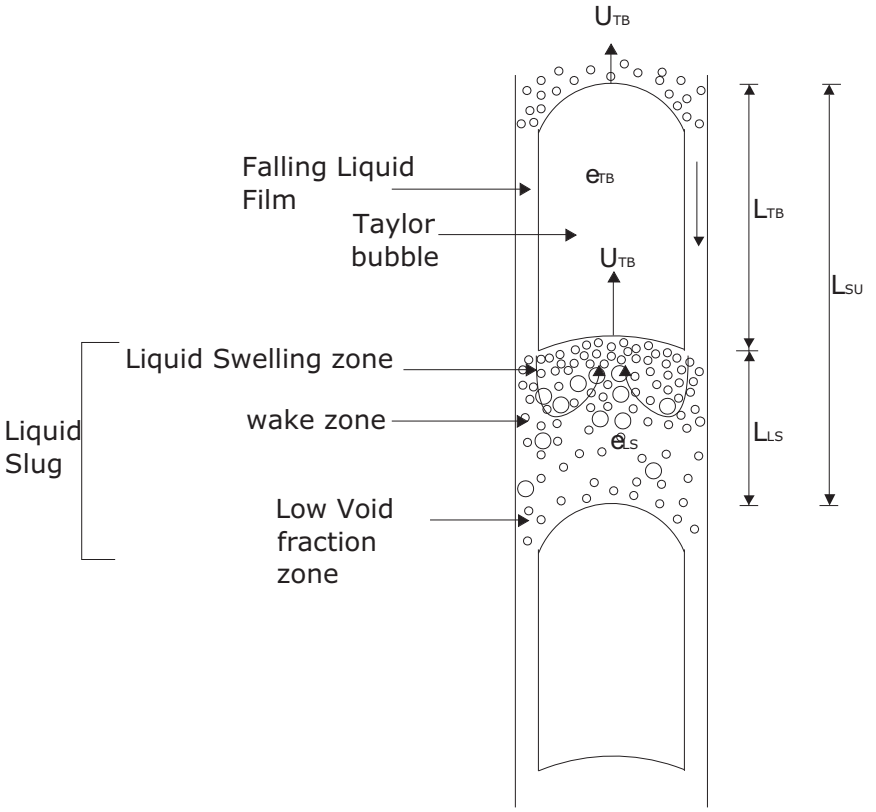

Figure 2: Schematic diagram of Slug flow structure

EXPERIMENTAL ARRANGEMENTS

The bubble column experimental set-up consists of a 50 mm internal diameter and 1.6 m long Perspex column in a vertical orientation. At the bottom of the column is a single nozzle gas distributor through which gas is introduced into the column. Two valves, V1 and V2 are used to control the flow of gas into the column and for the draining out of the liquid from the column respectively. The gas nozzle is connected to a flow meter of model Solartron Mobrey K5011927/2/JC/300 which measures the gas flow rate. A pressure gauge connected to the flow meter reads the pressure of the gas. A Phantom High Speed Video Camera was used to obtain the video of the gas-liquid flow in the column. A frame rate of 1000 pictures per second (pps) and exposure time of 100μs was used. The geometry specified gives the image width by image height as 512 by 512 pixel.

Fitted midway to the column is the twin Planes Electrical Capacitance Tomography (ECT) sensor with an interplanar spacing of 30mm as shown in Figure 3. The 8-electrodes system consists of measurement and driven guard electrodes of dimensions 2×8×29 mm which is connected to the Electrical Capacitance Tomography processor box, TFLR 5000-20 manufactured by Tomoflow Electronics. This sensor electronics gives 28 measurements which are relayed to the computer where image reconstruction occurs, and the data are acquired and processed to obtain the liquid holdup (which is the fraction of liquid in the gas-liquid mixture). The void fraction otherwise known as gas holdup is hence obtained from this.

The ECT is located about 0.7m above the nozzle, while the liquid level is located about 0.095m above the ECT sensor. On supplying the gas, the gas flows into the bubble column through the single nozzle gas distributor with an orifice diameter of 6.8mm. A range of silicone oil with viscosities 5, 100, 1000 and 5000 mPa.s were used.

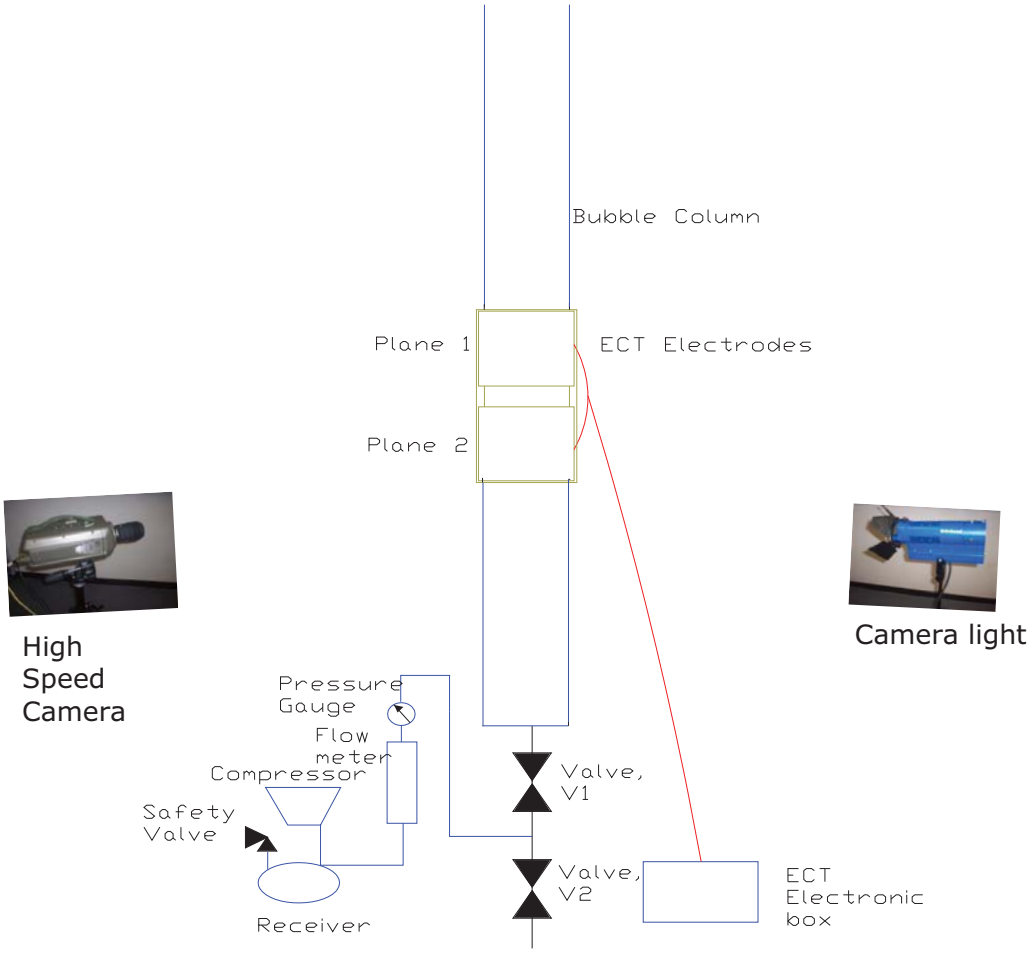

Figure 3: Schematic diagram of the 50mm diameter bubble column Experimental facility

With the use of the ECT sensor, it becomes possible to investigate slug flow in the column. The void fraction data from the ECT were obtained and analyzed to obtain the time series, probability density function (PDF) and power spectral density (PSD) through which the slug parameters such as length of Taylor bubbles and liquid slug, void fraction in Taylor bubbles and liquid slug, slug frequency, film thickness and pressure gradient in the slug were measured and analyzed. The ECT sensor used is shown in figure 4.

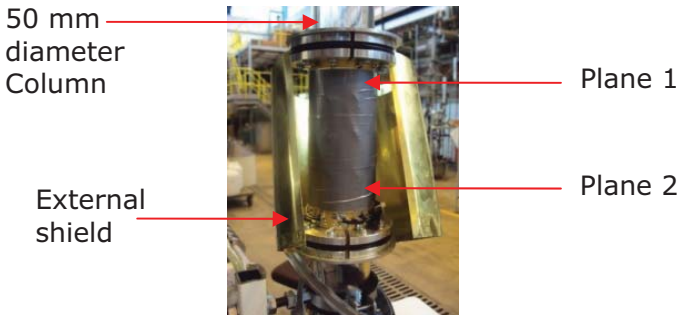

Figure 4: The twin-plane ECT sensor used

EXPERIMENTAL RESULTS AND ANALYSIS

Effect of viscosity on slug length

The effect of viscosity on the length of Taylor bubble and Liquid slug has been investigated using the equations presented by [1].

Length of slug unit, L_{SU} is given as;

$$\mathrm{L_{SU}} = \frac{\mathrm{U_N}}{\mathrm{f}} \tag{1}$$

Length of liquid slug, L_S is given as:

$$\mathrm{L_S} = \frac{\mathrm{L_{SU}}}{\mathrm{c+1}} \tag{2}$$

Where

$$\mathrm{c} = \frac{\mathrm{L_{TB}}}{\mathrm{L_{TB}}} = \frac{\mathrm{t_{TB}}}{\mathrm{t_s}} \tag{3}$$

Length of Taylor bubble is given as;

$$\mathrm{L_{TB}} = \mathrm{L_{SU}} - \mathrm{L_S} \tag{4}$$

Details of the derivations can be found in [1].

Length of Taylor bubble, $\mathrm{L_{TB}}$

The variation of length of Taylor bubble with superficial gas velocity is shown in figure 5.

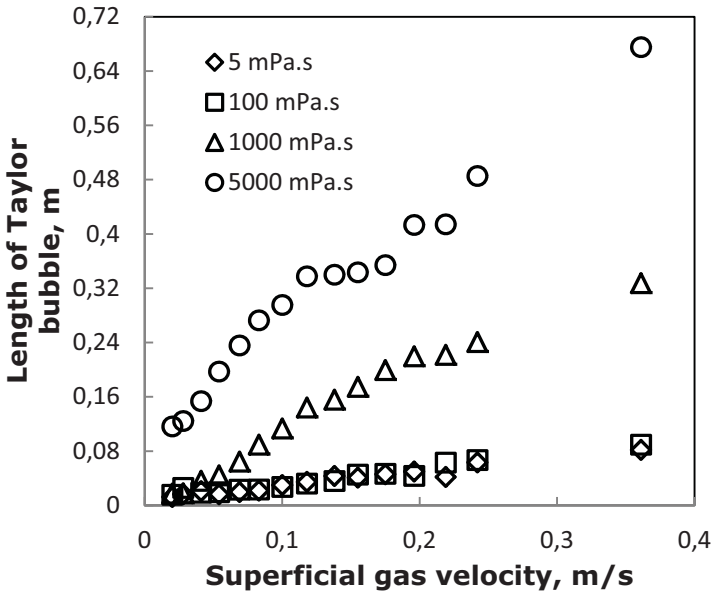

Figure 5: Variation in Length of Taylor bubble with superficial gas velocity at different viscosities

It is seen that as viscosity increases, the length of Taylor bubbles increases. This is due to the viscous effect which leads to bubble coalescence in high viscous liquids in the form of Taylor bubbles as superficial gas velocity increases. The lengths of Taylor bubbles for both 5 and 100 mPa.s were relatively the same. This is evident from their void fraction results which were relatively close which implies the fraction of gas in the gas-liquid mixture were quite the same. As superficial gas velocity increases in these two liquid

viscosities, small bubbles merge together causing an increase in bubble size as they rise due to a decrease in hydrodynamic static pressure with decreasing depth. Bubbles with different sizes where observed as seen in the high speed camera which leads to different rise velocities, which eventually leads to greater bubble collision than uniformly sized bubble. The growth of the bubbles by collision continues until some large bubbles begin to take the shape of a cap called spherical cap bubbles as seen in 5 and 100 mPa.s from a superficial gas velocity of 0.02 to 0.138 m/s. With further increase in superficial gas velocity from 0.155 to 0.361 m/s, there is the formation of deformed Taylor bubbles which also seem to cover a significant part of the column. This can be referred to as developing slug flow. It becomes developed with further increase in superficial gas velocity.

At a superficial gas velocity of about 0.02 m/s, the length of Taylor bubble of 1000 mPa.s assumes the same length with that of both 5 and 100 mPa.s, which now begins to increase drastically as superficial gas velocity increases. In essence, the initial Taylor bubble at low superficial gas velocity is that of a cap bubble which grows through collision between bubbles leading to coalescence. Also the small bubbles in the wake of the cap bubble travel faster until they are joined to the cap. The bubbles keep growing until they occupy a large part of the column cross-section thereby forming slugs. As viscosity increases from 1000 to 5000 mPa.s, the bubble size becomes larger due to coalescence leading to longer length of Taylor bubble. This implies that coalescence in viscous liquids is directly proportional to liquid viscosity.

$$\text{Liquid viscosity}, \mu \; \alpha \; \text{Length of Taylor bubble}, L \tag{5}$$

As liquid viscosity increases, bubble size increases with increase in bubble coalescence due to an increase in drag force. The trend obtained confirms the observation of [1] which is the increase in Taylor bubble with increase in superficial gas velocity. The initial and final length for all viscosities considered is shown in table 1 below:

Table 1: Initial and final length of Taylor bubble

Viscosity, μ (mPa.s)	Initial length of Taylor bubble at 0.02 m/s, (m)	Final length of Taylor bubble at 0.361 m/s, (m)
5	0.02	0.078
100	0.02	0.08
1000	0.02	0.32
5000	0.11	0.69

The length of the sensor cross-section is 0.232 m while the width is 0.058 m. Above a superficial gas velocity of 0.078 m/s and 0.24 m/s for 1000 and 5000 mPa.s respectively, the length of Taylor bubble exceeds that of the sensor length.

Another reason which may be responsible for the increase in length of Taylor bubble as viscosity increases is the wall effect. As viscosity increases, the impact by the walls of the column on the liquid increases which constrains it to assume the shape of a Taylor bubble. The shapes and sizes of the bubbles for the viscosities considered as seen from the high speed camera are shown in figure 6.

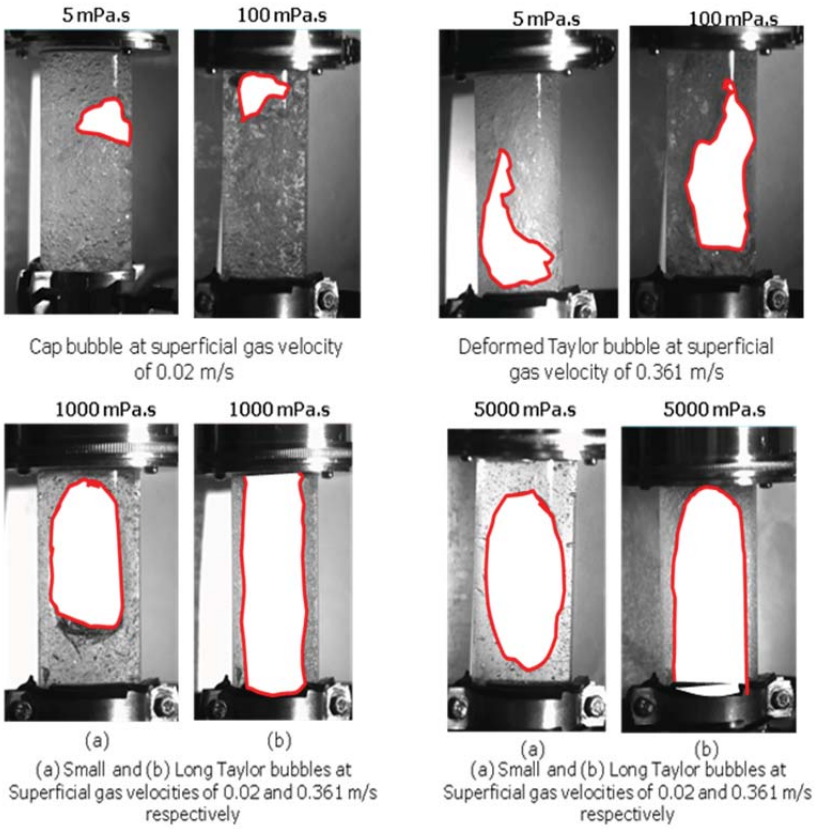

Figure 6: Variation of bubble size with increase in viscosity as superficial gas velocity increases

Length of Liquid Slugs, L_S

As the liquid viscosity increases, the length of the liquid slug decreases and gradually approaches zero at high viscosity. This is because in high viscous liquid, as gas superficial velocity increases, there is more of Taylor bubbles than liquid slug due to the fact that the viscous-controlling regime is dominating, which eventually leads to coalescence. The bigger bubbles entrained in the liquid slug merge with succeeding Taylor bubbles thereby provoking an increase in the length of the Taylor bubble and a decrease in the length of liquid slugs. For the 5 and 100 mPa.s liquid viscosities, values of the length of the liquid slugs are relatively close and it increases as gas superficial velocity increases from 0.02 to about 0.2 m/s and then starts to decrease slightly from a gas superficial velocity of 0.2 to 0.361 m/s. The decrease could be attributed to transition from spherical cap bubble to developing slug flow which appears as deformed Taylor bubbles as shown in Figure 6.

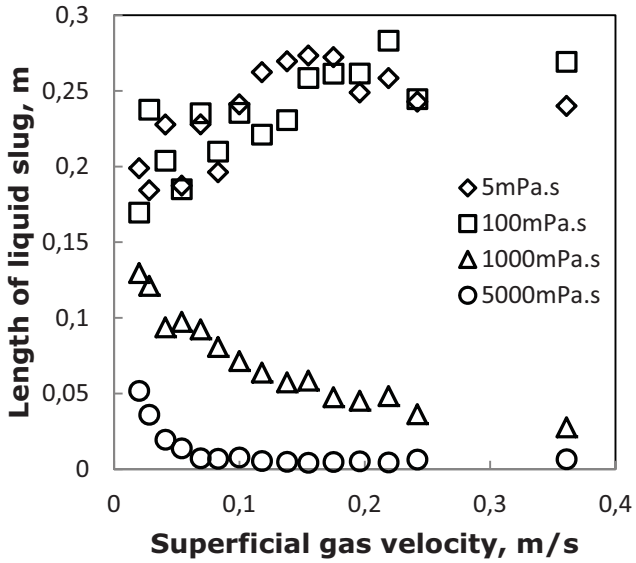

Figure 7: Variation in Length of liquid slug with superficial gas velocity at different viscosities

The initial, transition and final length of liquid slugs for all viscosities considered are shown in table 2.

Table 2: Initial, transition and final length of liquid slugs

Viscosity, μ (mPa.s)	Initial length of Liquid Slugs at 0.02 m/s, (m)	Transition length of liquid slugs at 0.2 m/s	Final length of Taylor bubble at 0.361 m/s, (m)
5	0.2	0.26	0.25
100	0.17	0.27	0.28
1000	0.14	_	0.03
5000	0.06	_	0.01

At a transition from spherical cap bubble to developing slug flow for liquid viscosities of 5 and 100 mPa.s, the length of liquid slugs are quite close. The final length of the liquid slug for a viscosity of 100 mPa.s is found to be slightly higher than that of 5 mPa.s. This could be due to the sensitivity of ECT instrument used to temperature changes. Changes in operating temperature can lead to measurement drift, which is one of the limitations of ECT [1].

The summary of the range of length of Taylor bubble and liquid slug for all viscosities considered for superficial gas velocities in the range 0.02 to 0.361 m/s is given in table 3, where D is the diameter of the column.

Table 3: Range of length of Taylor bubble and liquid slug

Viscosity, μ (mPa.s)	Length of Taylor bubble (m)	Length of Liquid slug (m)
5	0.25D-1.6D	3.7D-5.5D
100	0.32D-1.8D	3.4D-5.7D
1000	0.35D-6.5D	0.55D-2.6D
5000	2.3D-13.5D	0.09D-1D

It can be seen obviously from table 3 that length of Taylor bubble increases while length of liquid slug decreases with increase in viscosity. [22], [12], [11] and [13] specified the mean length of liquid slugs in vertical flow to be approximately in the range of 8-2D [10]. [22] gave stable liquid slug length of 6D-8D; [32], 30D-48D; [34], approximately 16D and [11], approximately 21.7D. This is dependent on the viscosity and range of gas superficial velocity used. The short length of liquid slugs observed in this work could be due to the use of higher liquid viscosities and low range of gas superficial velocities.

Effect of viscosity on void distribution in the slugs

The effect of viscosity on void fraction in Taylor bubble and liquid slugs has been studied. Void fraction in Taylor bubbles and liquid slugs were obtained through the application of statistical analysis on time-averaged void fraction data obtained from ECT using the Probability density function (PDF). The PDF is used to identify flow pattern and can be used to deduce the void fraction distribution in the slugs. If we define a function P(x)dx in which the data x(t) lies on the value between x and x+Δx, we have:

$$P(x)dx = P(x < x(t) \leq x+\Delta x) \quad (6)$$

The total area enclosed by this function is 1.

$$P(-\infty<x\infty) = \int_{-\infty}^{\infty} P(x)dx \equiv 1 \quad (7)$$

[5] gave the criteria for identification of flow pattern. For spherical cap bubble, the PDF trace of void fraction shows a single peak with a broadening tail extending to higher void fractions; while for slug flow, there exists two peaks with the high void fraction peak for Taylor bubble and the low void fraction peak for liquid slug. An example is the PDF of void fraction trace for 1000 mPa.s at a superficial gas superficial velocity of 0.069 m/s as shown in Figure 8.

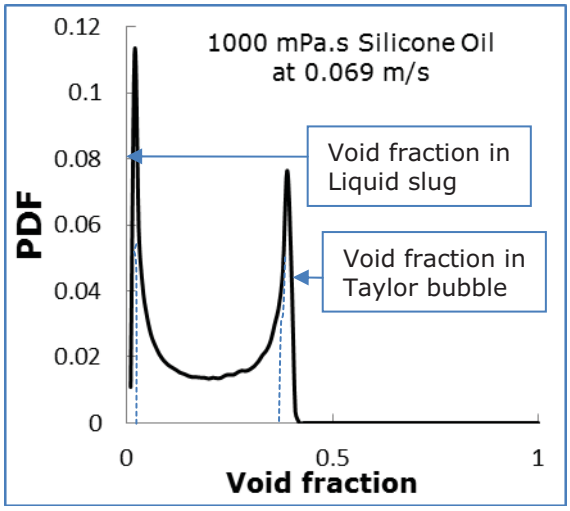

Figure 8: PDF trace of 1000 mPa.s at a superficial gas velocity of 0.069 m/s. The void fraction in Taylor bubble and liquid slugs are indicated.

Void fraction in liquid slugs

As gas superficial velocity increases, void fraction in liquid slugs increases and is more pronounced in 5 and 100 mPa.s viscosities. This confirms the work of [1] for 67 mm pipe and [26] for 38 mm pipe. As viscosity increases, void fraction in the liquid slug decreases and gradually approaches zero. This is due to the merging of the entrained big bubbles in the liquid slug with the succeeding Taylor bubbles leading to an increase in the length of Taylor bubbles and a decrease in the length and void fraction in the liquid slug. This also accounts for the trend obtained in the plot of length of liquid slug against gas superficial velocity. It could also be due bubble entrainment from the liquid film into the liquid slug due to the force of gravity. The plot of void fraction in liquid slugs with gas superficial velocity is shown in Figure 9.

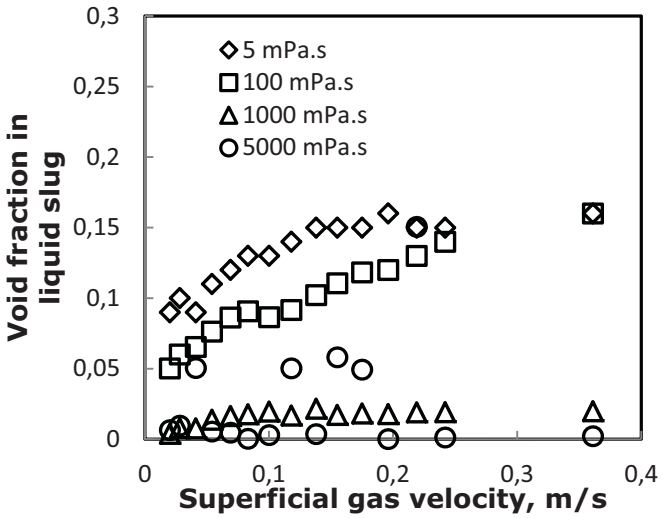

Figure 9: Variation of void fraction in liquid slug with superficial gas velocity at different viscosities. The four anomalous points of 5000 mPa.s indicates bubble entrainment in liquid slug

The void fractions of 5000 mPa.s at some points were found to be increase. This is due to the breakup of Taylor bubbles which could be through fragmentation of the bubble tail which makes small gas bubbles to be entrained in the liquid slug. This confirms what was reported by [10]. It could also be as a result of gravity which forces the liquid in the liquid film to fall and impinge the liquid slug thereby leading to flow separation at the bubble tail [10]. The result obtained also confirms the work of [2] and [24].

The initial and final void fraction in liquid slugs for all viscosities considered in this work is shown in table 4.

Table 4: Initial and final void fraction in liquid slugs

Viscosity, μ (mPa.s)	Initial void fraction at 0.02 m/s	Final void fraction at 0.361 m/s
5	0.09	0.161
100	0.055	0.16
1000	0.01	0.028
5000	0.005	0.005

Void fraction in Taylor bubbles

There is no clearly defined trend in the plot when all the viscosities are combined, but they become more meaningful when considered independently. The void fraction in the Taylor bubble for 5 and 100 mPa.s within superficial gas velocities of 0.02 to 0.155 m/s fall below that of 1000 and 5000 mPa.s. This is definitely due to the initial appearance of spherical bubbles cap bubbles in 5 and 100 mPa.s which are of low void fraction compared with 1000 and 5000 mPa.s, followed by the formation of deformed Taylor bubbles, which are of higher void fraction between 0.175 to 0.361 m/s, as shown in figure 6 and 10.

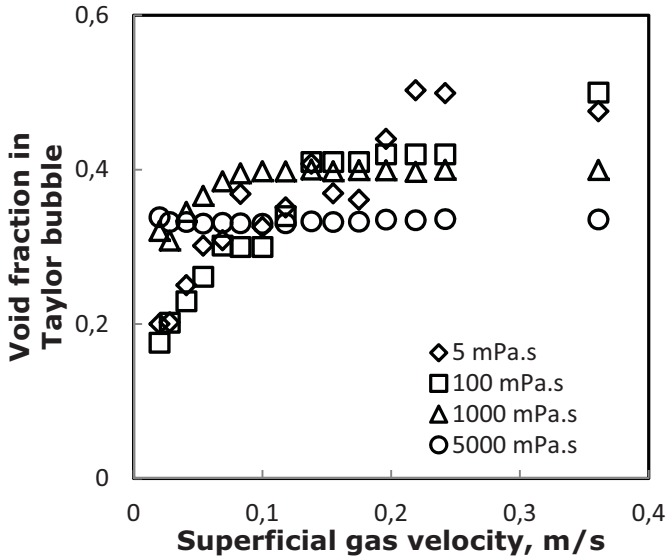

Figure 10: Variation of void fraction in Taylor bubble with superficial gas velocity at different viscosities.

The void fraction in Taylor bubble for 5 and 100 mPa.s gave similar trend with a corresponding increase with increase in gas superficial velocity. This is in agreement with the work of [1] in which 5 mPa.s viscosity was used. The void fraction tends to fall apart

from gas superficial velocity of 0.2 to 0.361 m/s with higher values of 5 mPa.s. This is probably due to the collapsing of the Taylor bubbles in the 100 mPa.s within the gas superficial velocity of 0.196 to 0.361 m/s. In the 1000 and 5000 mPa.s, the void fraction in the Taylor bubble increases and eventually stabilizes with an increase in gas superficial velocity. It can be concluded that as the gas superficial velocity increases in viscous liquids, a point is reached when there is no significant change in the void fraction of the Taylor bubble. At this point, coalescence rate becomes relatively constant.

For liquid viscosities of 5 and 100 mPa.s and for gas superficial velocities of 0.02 to 0.125 m/s, the flow pattern is spherical cap bubble. This may be the reason behind the irregular pattern observed as compared to 1000 and 5000 mPa.s. Between 0.17 and 0.361 m/s, deformed Taylor bubbles are formed. So, it becomes imperative to consider the ideal trend from 0.17 to 0.361 m/s of 5 and 100 mPa.s and 0.02 to 0.361 m/s of 1000 and 5000 mPa.s. This reveals that the void fraction in Taylor bubble decreases with an increase in viscosity. A close look at the plot when considered in terms of less viscous liquid only (i.e. 5 and 100 mPa.s) and more viscous liquid only (i.e. 1000 and 5000 mPa.s), also reveals that the void fraction in Taylor bubble decreases with an increase in viscosity. This is in contrast to the empirical correlation proposed by [2]. This can be attributed to the fact that they used air-water and air-kerosene mixtures as their model fluids. The viscosities (water viscosity = 0.890 mPa.s; kerosene viscosity = 1.64 mPa.s) used were quite low compared to those considered in this work. Hence, inertia forces are controlling rather than viscous forces.

The effect of viscosity on void fraction in Taylor bubbles can be further explained using a dimensionless number called Capillary Number as shown in figure 11. It gives the relative effect of viscous forces versus surface tension acting across a gas-liquid interface. It is expressed as:

$$\mathrm{Ca} = \frac{\mu_L U_{SG}}{\sigma_L} \tag{8}$$

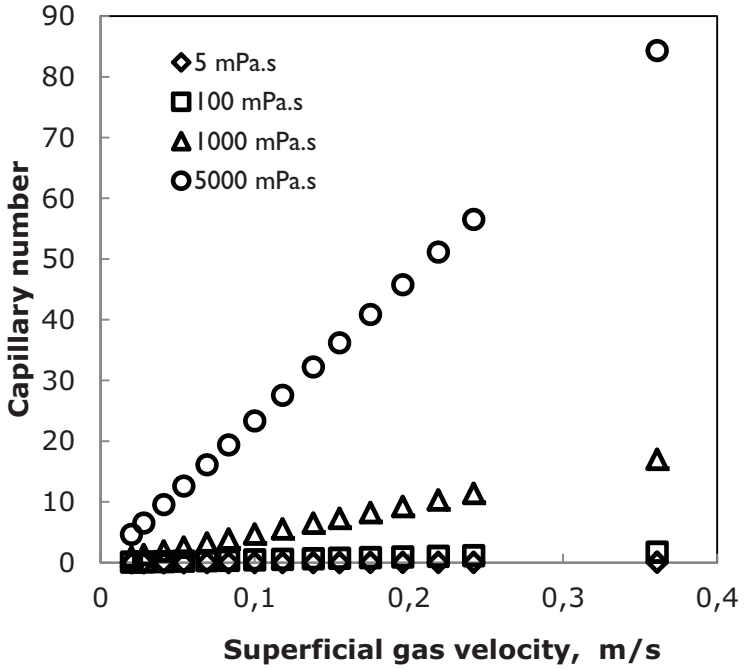

Figure 11: Effect of Capillary Number on Void fraction in Taylor bubble

Capillary number was observed to increase with increase in viscosity taking gas superficial velocity as a parameter. This shows the domineering effect of viscous force over surface tension force. The surface tension force helps to hold the bubbles together due to the force of cohesion forming an agglomerate of bubbles in the form of Taylor bubble. So, if the viscous force has a domineering effect over the surface tension force, the void fraction in Taylor bubble will tend to decrease as viscosity increases.

Effect of viscosity on Liquid Film

Thin film of liquid exists around the Taylor bubble. The thickness of this film is a function of the liquid viscosity which has been studied in this work.

Liquid Film Thickness

The effect of viscosity on film thickness has been evaluated using the correlation proposed by [7] which gives a geometrical relation between film thickness, δ and void fraction in the Taylor bubble, ε_B. This is given as:

$$\delta = \frac{D}{2}\left(1 - \varepsilon_{TB}^{\frac{1}{2}}\right) \quad (9)$$

On plotting the film thickness against the superficial gas velocity, the trend obtained is shown in figure 12.

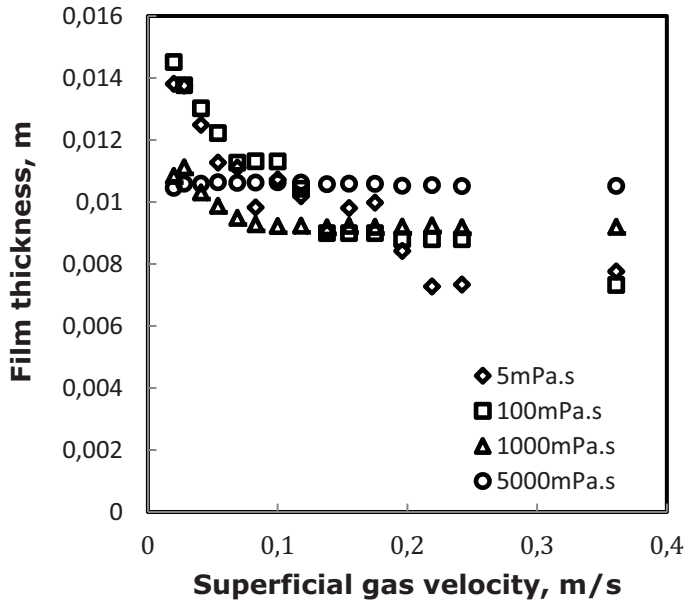

Figure 12: Variation of Film thickness with superficial gas velocity at different viscosities.

Figure 12 shows no clearly defined trend from 5 to 5000 mPa.s. This is due to the appearance of spherical cap bubbles between 0.02 and 0.175 m/s superficial gas velocities, which has no liquid film associated with it unlike the case of Taylor bubbles. From 0.196 to 0.361m/s, there is the formation of liquid film around the deformed Taylor bubbles with the thicknesses falling below that of 1000 mPa.s. It can be concluded that the liquid film thickness increases with an increase in liquid viscosity. This is probably due to the effect of the interfacial and wall shear forces. The interfacial and wall shear forces increases as viscosity increases, which lead to increasing shearing off of the liquid from the gas which culminates in increasing accumulation of liquid film on the wall. In essence, entrained liquid in the gas bubbles is deposited in the liquid film. It can be observed from

the plot that the liquid film thickness decreases with an increase in gas superficial velocity. This is because as gas superficial velocity increases, the bubble diameter also increases hence, an increase in the area covered by the bubble within the column cross-section. This causes a corresponding decrease in the layer of liquid film around the Taylor bubble. The decrease of the liquid film thickness becomes quite minimal as gas superficial velocity increases.

Effect of viscosity on Pressure Gradient in Slug

The overall pressure gradient in the slug unit is dependent on three components: gravitational, frictional and acceleration pressure gradient. The [7] model has been adopted to evaluate these. The pressure gradient is given as:

$$\frac{dP}{dz} = \left(\frac{dP}{dz}\right)_g + \left(\frac{dP}{dz}\right)_f + \left(\frac{dP}{dz}\right)_a \tag{10}$$

with a neglection of gas weight and momentum, where z is the height above the air-injection nozzle.
The analysis of [36] has been used to obtain the gravitational and frictional components of the pressure gradient.

Gravitational pressure gradient component
This acts downwards in the column. The liquid slug and falling liquid film both contribute to the gravitational component of the pressure gradient. Hence, the average gravitational component is given as:

$$\left(\frac{dP}{dz}\right)_g = \text{liquid slug term} + \text{falling film term} \tag{11}$$

Which is further expressed as:

$$\left(\frac{dP}{dz}\right)_g = \rho_L g\left[(1-\beta) + (1-\varepsilon_{TB})\right] \tag{12}$$

Where the first and second terms represent the liquid slug and falling liquid film respectively.

Frictional pressure gradient component
This is dependent on the pressure gradient due to the liquid slug and the Taylor bubble. In the region of the Taylor bubble, when the liquid film becomes fully developed, its weight is fully balanced by the wall friction force.
The average frictional component is hence given as:

$$\left(\frac{dP}{dz}\right)_f = \left((1-\beta)\left(\frac{dP}{dz}\right)_{fs}\right) + \beta\left(\frac{dP}{dz}\right)_{fB} \tag{13}$$

Where, the friction term of the liquid slug is given as:

$$\left(\frac{dP}{dz}\right)_{fs} = -\frac{\lambda_j \rho_L U_m}{2D} \tag{14}$$

$$U_m = U_{SG} + U_{SL} \tag{15}$$

λ_j is the friction factor which is obtained from the Blasius' formula.

$$\lambda_j = 0.316\mathrm{Re}^{-0.25} \tag{16}$$

This Reynolds number is dependent on the superficial gas velocity, U_{SG}.

$$\mathrm{Re} = \frac{\rho_L U_{SG} D}{\mu_L} \tag{17}$$

The friction term of the Taylor bubble is given as:

$$\left(\frac{dP}{dz}\right)_{fB} = \rho_L g(1-\varepsilon_{TB}) \tag{18}$$

[7] reveals that the model used does not account for the transition between the rising liquid slug and the falling liquid film (the liquid around the Taylor bubble nose).

Acceleration Pressure Gradient component

This is the pressure gradient required to reverse the direction and accelerate the liquid film falling around the Taylor bubble to the velocity of liquid in the liquid slug [33]. The contribution of this component to the overall pressure gradient is quite small. This is given as:

$$\left(\frac{dP}{dz}\right)_f \approx \rho_L \frac{d}{dz}\left[V_L^2(1-\varepsilon)\right] = \rho_L U_{SL}^2 \frac{d}{dz}\left(\frac{1}{1-\varepsilon}\right) \tag{19}$$

The void fraction is given as:

$$\varepsilon = \frac{U_{gs}}{V_G} = \frac{U_{gs}}{C_o U_m + V_o} \tag{20}$$

Assuming the gas behaves as ideal gas,

$$\rho_G = \rho_{Gr}\frac{P}{P_r} \tag{21}$$

Where ρ_{Gr} is the gas density at a reference pressure, P_r.

Merging equation (21) and (20) with (19) to evaluate the overall pressure gradient gives:

$$\frac{dP}{dz} = \alpha\left[\left(\frac{dP}{dz}\right)_g + \left(\frac{dP}{dz}\right)_f\right] \tag{22}$$

Where α is the acceleration correction factor given as:

$$\alpha = \left[1 - \rho_L U_{SL}^2 \frac{U_{SG}(C_o U_{SL} + V_o)}{P[(C_o-1)U_{SG} + C_o U_{SL} + V_o)]^2}\right]^{-1} \tag{23}$$

In this work, the liquid is stagnant, hence $U_{SL} = 0$, which gives $\alpha = 1$. So, the acceleration pressure gradient becomes zero.

The plot of Overall pressure gradient against the superficial gas velocity is shown in figure 13.

It can be seen from this plot that overall pressure gradient increases as viscosity increases with an increase of gas superficial velocity as a parameter. The overall pressure gradient associated with the silicone oil of viscosities of 5 and 100 mPa.s are quite close. This is quite evident from the close void fraction data.

Pressure gradient can be said to be the change in resultant forces acting in the column per unit change in cross-sectional area in the slug. These forces are frictional,

gravitational and acceleration forces, with the acceleration forces being negligible due to the stagnant liquid in the column. For each viscosity considered, as superficial gas velocity increases, overall pressure gradient in the slug increases. As viscosity increases, the slug cross-sectional area increases with an increase in the frictional and gravitational forces impacting on the slug. This increase in frictional and gravitational forces impacting on the slug results into an increase in frictional and gravitational pressure gradient; hence, an increase in the overall pressure gradient. The increase in the slug cross-sectional area is due to the increase in the diameter of slug as viscosity increases. This increase in slug diameter is as a result of coalescence.

The pressure gradient is observed to be negative because the friction term is the opposite of the gravity term. Hence, the frictional pressure gradient is positive whilst that of gravitational is negative which eventually leads to negative pressure gradient. As viscosity increases from 1000 to 5000 mPa.s, overall pressure gradient in the slug tends to zero.

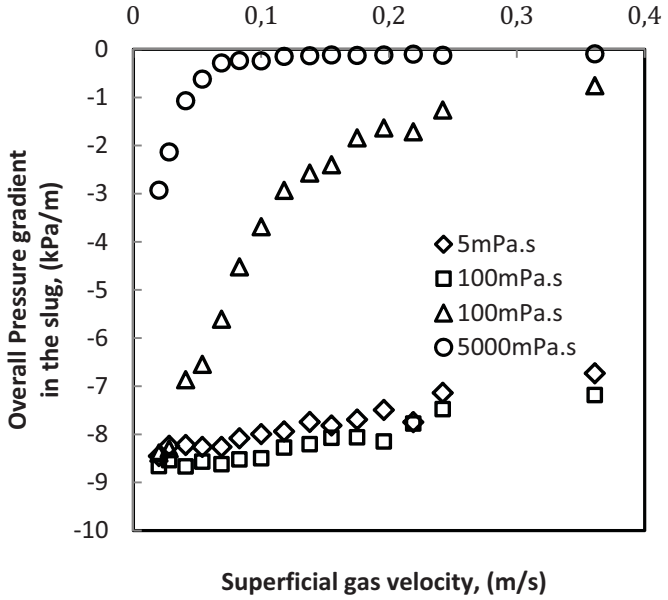

Figure 13: Pressure gradient for different viscosities

Effect of viscosity on structure Velocity

This is the rise velocity of the Taylor bubble which is expressed as a linear relationship with the mixture velocity according to [25] using air-water system. This is given as:

$$V_G = C_o U_m + V_o \quad (24)$$

The structure velocity is obtained by the cross correlation between two planes - plane 1 and plane 2 using the time-averaged void fraction data obtained from ECT.

The plot of structure velocity against superficial gas velocity for various viscosities is shown in figure 14.

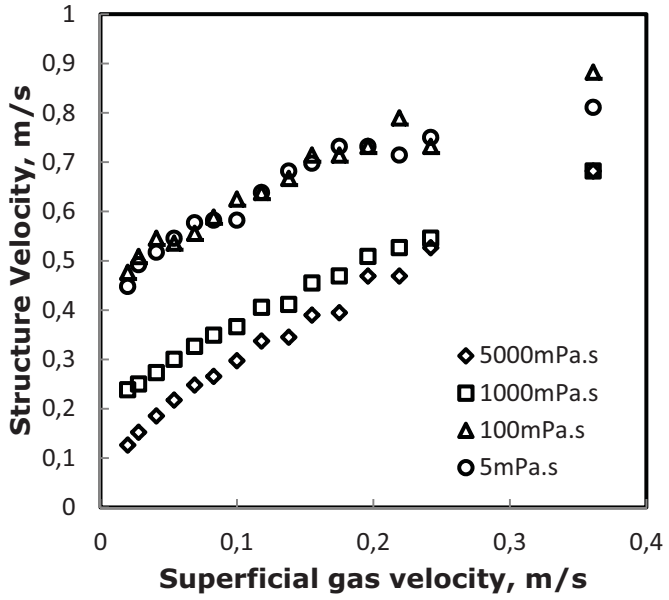

Figure 14: Variation of Structure velocity with superficial gas velocity at various viscosities

From the plot, structure velocity increases with increase in superficial gas velocity. This is in agreement with [1]. It can also be observed that the structure velocity decreases with increase in viscosity. This can be attributed to viscous effect which can be explained based on the dimensionless fluid property numbers: Morton number, Eotovos number, dimensionless inverse viscosity and the Reynolds number. According to [21], the dimensionless inverse viscosity is directly proportional to the fourth root of the Eotovos number raised to a power of three and inversely proportional to the fourth root of the Morton number. Morton number, M_o is used alongside with Eotovos number, E_o to characterize the shape of bubbles or drops moving in a surrounding fluid or continuous phase.

Morton number is given as:

$$M_o = \frac{g\mu_L^4}{\rho_g \sigma_L^3} \tag{25}$$

Eotovos number is given as:

$$E_o = \frac{\rho g D}{\sigma_L} \tag{26}$$

The dimensionless inverse viscosity is given as:

$$N_f = \left(\frac{E_o^3}{M_o}\right)^{1/4} \tag{27}$$

From the various viscosities considered, the property numbers are given as follows:

For 5mPa.s, $M_o = 8.7645 \times 10^{-7}$; $E_o = 1139.105$; $N_f = 6408.267$;
For 100mPa.s, $M_o = 1.11353 \times 10^{-5}$; $E_o = 1132.374$; $N_f = 337.9223$;
For 1000mPa.s, $M_o = 1061.426$; $E_o = 1122.134$; $N_f = 33.96732$;
For 5000mPa.s, $M_o = 644964.7$; $E_o = 1111.647$; $N_f = 6.793463$;

It will be observed that as viscosity increases, Morton number, M_o increases while the Eotovos number, E_o decreases which culminates in the decrease of the dimensionless inverse viscosity. As the dimensionless inverse viscosity decreases, viscous effect dominates.

According to [37], viscous effects come into play when the square of dimensionless inverse viscosity, N_f is less than 3×10^5. This is given as:

$$(N_f)^2 = \frac{(\rho_L^2)gD^3}{\mu_L^2} < 3 \times 10^5 \quad (28)$$

For 5mPa.s, $(N_f)^2$ = 41012747;
For 100mPa.s, $(N_f)^2$ = 114051.4;
For 1000mPa.s, $(N_f)^2$ = 1152.37;
For 5000mPa.s, $(N_f)^2$= 46.09481

The 100mPa.s, 1000mPa.s and 5000mPa.s satisfy the condition of $(N_f)^2 < 3 \times 10^5$ which implies viscous effect dominates.

Reynolds number is inversely proportional to viscosity, $\mathrm{Re} \propto \frac{1}{\mu}$ and also inversely proportional to viscous forces.

$$\text{i.e. } \mathrm{Re} = \frac{\text{Inertial forces}}{\text{Viscous forces}} \quad (29)$$

So, as viscosity increases, the Reynolds number decreases, hence viscous forces dominate. This can be seen from the Reynolds number values of 5, 100, 1000 and 5000mPa.s silicone oil at a superficial gas velocity of 0.02m/s, which are 183, 9.65, 0.97 and 0.194 respectively. As Reynolds number increases, viscous effect will be negligible while as Reynolds number decreases, viscous effect becomes dominant. So, viscous effect increases with decrease in Reynolds number. The drag coefficient, a dimensionless quantity used to quantify the drag or resistance of an object in a fluid environment is inversely proportional to the Reynolds number given as:

$$C_D = \frac{24}{\mathrm{Re}} \quad (30)$$

So, as the Reynolds number decreases, the drag coefficient increases due to viscous effect.

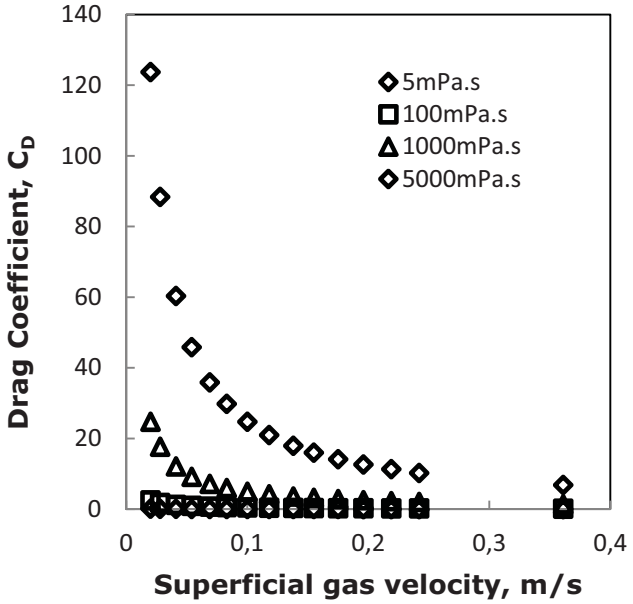

Figure 15: Drag Coefficient versus Superficial gas velocity

From the plot of Drag Coefficient versus the superficial gas velocity for different viscosities of 5, 100, 1000 and 5000mPa.s silicone oil, as viscosity increases, the drag coefficient increases which implies that the motion of the bubble through the liquid is

hindered leading to a decrease in the structure velocity. Also, from Stokes law, drag force is given as:

$$F_D = 3\pi\mu Vd \tag{31}$$

This is based on the fact that the flow is laminar.
Introducing equation (14) into (15) gives:

$$F_D = \frac{72\pi\mu^2}{C_D\rho} \tag{32}$$

From equation (15), the drag force is directly proportional to viscosity, $F_D \alpha\, \mu$ which implies that as viscosity increases, drag force otherwise called fluid resistance increases. This is confirmed by the plot shown below:

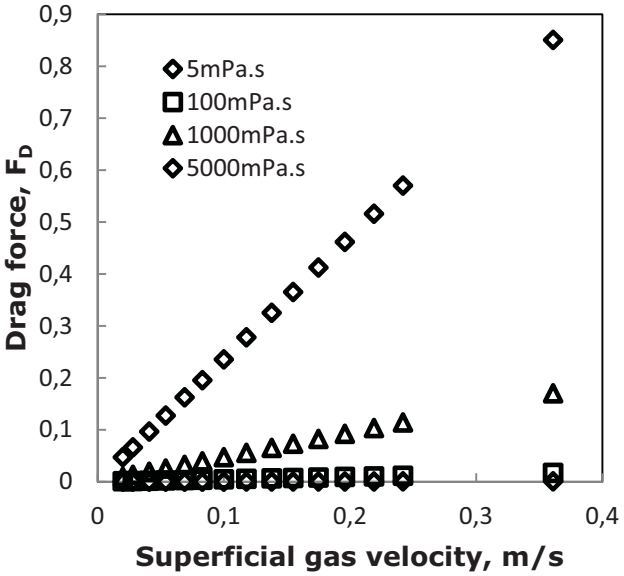

Figure 16: Drag force versus Superficial gas velocity

The figure (16) above shows that as viscosity increases, there is a linear increase in drag force. This increase in viscosity constitutes a viscous effect. The drag force opposes the motion of the bubbles through the liquid acting parallel to the direction of relative motion, making them to proceed at a much slower rate. Hence, the decrease in the structure velocity with increase in viscosity.

From the linear expressions obtained from the structure velocity plots, we have:

For 5 mPa.s, $V_G = 1.0763U_{gs} + 0.4899$ (33)
For 100 mPa.s, $V_G = 1.1825U_{gs} + 0.4893$ (34)
For 1000 mPa.s, $V_G = 1.3228U_{gs} + 0.2306$ (35)
For 5000 mPa.s, $V_G = 1.6118U_{gs} + 0.1254$ (36)

This implies that as viscosity increases, the distribution coefficient increases (from 1.0763 to 1.6118) while the drift velocity decreases (from 0.4899 to 0.1254 m/s).

Effect of viscosity on Slug frequency

The Slug frequency, f is given as:

$$f = \frac{U_N}{L_{SU}} \tag{37}$$

Where U_N is the structure velocity, and L_{SU}, the length of slug unit.

It is the number of slugs passing through the column cross-section over a certain period of time. It is obtained through statistical analysis using the power spectral density (PSD) technique. This involves the computation of the Fourier Transform of the auto correlation sequence of the time series from either plane. As the gas superficial velocity increases, slug frequency increases. This is in agreement with [1]. The bubble frequencies for both 5 and 100 mPa.s were quite close most especially at a gas superficial velocity of 0.17 to 0.361 m/s. This range indicates a developing slug and the number of slugs at this region are the same. With an increase of viscosity from 5 to 5000 mPa.s, slug frequency can be observed to decrease. This is accounted for by the dominating effect of viscous forces over inertia forces. This constitutes the viscous effect which leads to an increase in drag force and a subsequent decrease in the bubble rise velocity, with the length of slug unit increasing due to coalescence, hence a decrease in bubble frequency as liquid viscosity increases. This is contrary to what was proposed by [15]. This is probably due to the use of horizontal pipe. The length of slug unit increases with an increase in viscosity which reduces the amount of bubbles captured within the sensor's cross-section over a period of time (bubble frequency).

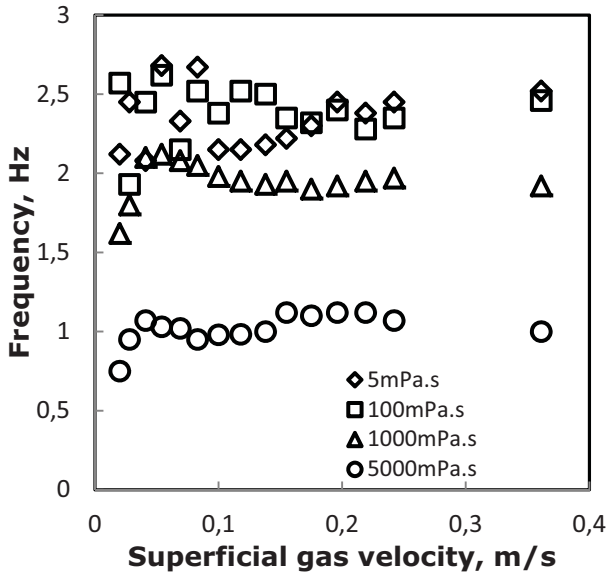

Figure 17: Variation of Frequency with superficial gas velocity at various viscosities

CONCLUSIONS

The effect of viscosity on slug flow has been studied and analyzed using Electrical Capacitance Tomography instrumentation and the high speed video camera. From the results of this study, the following conclusions can be drawn:

Conclusion for the effect of viscosity on slug flow

The effect of viscosity on slug flow has been studied and analyzed using Electrical Capacitance Tomography and high speed video camera. From the results of this study, the following conclusions can be drawn:

(1) The length of Taylor bubble increases whilst the length of the liquid slug decreases as viscosity increases. This is due to the viscous controlling regime which subsequently leads to coalescence.
(2) The void fraction in Taylor bubbles and liquid slug decreases as viscosity increases. This is majorly due to coalescence, in which for the latter, entrained

big bubbles in the liquid slug merge with the succeeding Taylor bubbles. The decrease in void fraction in Taylor bubbles as viscosity increases could also be attributed to the domineering effect of viscous force over the surface tension force.

(3) Liquid film thickness increases as viscosity increases due to the effect of interfacial and wall shear forces.
(4) Slug frequency and structure velocity were found to decrease with increases in viscosity due to the dominating effect of viscous forces over inertia forces with an increase in drag force.
(5) The pressure gradient associated with the slug increases as viscosity increases. This is majorly due to an increase in slug cross-sectional area and the increase in frictional and gravitational forces impacting on the slug.

ACKNOWLEDGEMENTS

Kajero O.T., will like to appreciate the Nigerian government through the Education Trust Fund (ETF) for sponsoring his doctoral studies.

NOMENCLATURE

ε_B = Mean void fraction, dimensionless
L_{TB} = Length of Taylor bubble, m
L_{LS} = Length of Liquid Slug, m
L_{SU} = Length of Slug unit, m
ε_{TB} = Void fraction of the Taylor bubble
ε_{LS} = Void fraction of the liquid slug
U_{TB} = Velocity of Taylor bubble, m/s
f = frequency of bubbles, Hz
μ_L = liquid viscosity, kg/m.s
D = Column diameter, m
δ = Film thickness, m
d_o = orifice diameter, m
σ_L = surface tension (N/m)
ρ_L = liquid density, kg/m^3
g = acceleration due to gravity, m/s^2
Q = gas flow rate, m^3/s
$\frac{dP}{dz}$ = overall pressure gradient, Pa/m
$\left(\frac{dP}{dz}\right)_g$ = gravitational pressure gradient, Pa/m
$\left(\frac{dP}{dz}\right)_f$ = frictional pressure gradient, Pa/m
$\left(\frac{dP}{dz}\right)_a$ = acceleration pressure gradient, Pa/m
β = ratio of length of Taylor bubble to slug unit, dimensionless
$\left(\frac{dP}{dz}\right)_{fs}$ = frictional pressure gradient in the liquid slug, Pa/m
$\left(\frac{dP}{dz}\right)_{fB}$ = frictional pressure gradient in the Taylor bubble, Pa/m
U_m = mixture velocity, m/s
U_{SG} = superficial gas velocity, m/s
U_{SL} = superficial liquid velocity, m/s
λ_j = friction factor, dimensionless
Re = Reynolds number, dimensionless
E_o = Eotovos number, dimensionless

Fr = Froude's number, dimensionless
M_o = Morton number, dimensionless
N_f = Inverse dimensionless viscosity, dimensionless
ρ_{Gr} = gas density at a reference pressure, P_r
α = acceleration correction factor, dimensionless
V_o = drift velocity, m/s^2
C_o = distribution coefficient, dimensionless
ρ_G = gas density, kg/m^3
C_D = drag coefficient, dimensionless
F_D = drag force, N

REFERENCES

[1] Abdulkadir M., Hernandez-Perz V., Abdulkareem L., Lowwndes I.S and Azzopardi B.J.: Characteristics of slug flow in a vertical riser, SPE 140681, 2010.

[2] Abdul-Majeed G.H.: Liquid slug holdup in horizontal and slightly inclined two-phase slug flow, Journal of Petroleum Science and Engineering 27, 2000, pp. 27–32.

[3] Azzopardi, B.J.: Gas–Liquid Flows, Begell House Inc, New York, 2006.

[4] Brauner N. and Ullman A.: Modelling of gas entrainment from Taylor bubbles. Part A: Slug flow, International Journal of Multiphase Flow, 30, 2004, 239-272.

[5] Costigan G. and Whalley P.B.: Slug Flow Regime Identification from Dynamic void fraction measurements in vertical air-water flows, Int. J. Multiphase Flow, Vol. 23, No. 2, 1997, pp. 263-282.

[6] Crowley C.J., Sam R.C., Wallis G.B. and Metha D.C.: Slug flow in a large diameter pipe: 1. Effect of fluid properties, AIChE Annual Meeting, San Francisco, CA, 1984.

[7] De Cachard F. and Delhaye J.M.: A slug-churn flow model for small diameter airlift pumps, International Journal of Multiphase flow, No. 4, 1996, pp. 627-649.

[8] Deckwer W., Louisi Y., Zaidi A and Ralek M.: Hydrodynamic properties of the Fischer-Tropsch Slurry Process, Industrial Engineering Chemical Process Description Development, 19, 1980, 699-709.

[9] Deckwer W.D.: Bubble Column Reactors, Chichester, Wiley, 1992.

[10] Fabre J. and Line A.: Modeling of Two-phase Slug flow, Annual Review of Fluid Mechanics, 24: 1992, 21-46.

[11] Fernandes, R.C.: Experimental and theoretical studies of isothermal upward gas-liquid flows in vertical tubes, PhD thesis, Univ. Houston, 1981.

[12] Fitremann, J.M.: Ecoulements diphasiques: theorie et application a l'etude de quelques regimes d'ecoulements verticaux ascendants d'un melange gaz-liquide. These Univ. Pierre et Maric Curie, Paris, 1977.

[13] Frechou, D.: Etude de l'ecoulement ascendant a trios fluids en conduit vertical. These Inst. Natl. Polutech., Tolulouse, 1986.

[14] Gaddis E.S. and Vogelpohl A.: Bubble formation in Quiescent liquids under constant flow conditions, Chemical Engineering Science, Vol. 41, No. 1, 1986, pp. 97-105.

[15] Gokcal B., Al-Sarkhi A.S, and Sarica C.: Prediction of slug frequency for high viscosity oils in horizontal pipes, SPE 124057, 2009.

[16] Hemdel T.J, Su X., Hol. P.D., Talcott S.M., and Staudt A.K.: The effect of bubble column diameter on gas holdup in fiber suspensions, Chemical Engineering Science, 61, 2006, 3098-3104.

[17] Kaji R., Azzopardi B.J., Lucas D.: Investigation of flow development of co-current gas liquid vertical slug flow, International Journal of Multiphase flow, 35, 2009, 335-348.

[18] Kantarci N., Borak F. and Ulgen K.O.: Review: Bubble Column Reactors, Process Biochemistry, 40, 2005, 2263-2283.

[19] Krishna R., Van Baten J.M., Urseanu M.I.: Scale effects on the hydrodynamics of bubble columns operating in the homogeneous flow regime, Chemical Engineering and Technology, 24(5), 2001, 451-458.
[20] Kumar S.B., Moslemian D. and Dudukovic M.P.: Gas-holdup Measurements Bubble Column using computed Tomography, AIChE Journal, June, Vol. 43, No. 6, 1997.
[21] Lu X. and Prosperetti A.: A Numerical Study of Taylor bubbles, Ind. Eng. Chem. Res., 48(1), 2009, pp. 242-252.

[22] Moissis, R. and Griffith, P.: Entrance effects in a two-phase slug flow, Journal of Heat Transfer, Transactions of the ASME, Series C 2, 1962, 29–39.
[23] Mori K., Kaji M., Miwa M. and Sekoguchi K.: Interfacial structure and void fraction of slug flow for upward gas-liquid two-phase flow, Two-phase flow Modeling and Experimentation (Ed. G.P. Celata, P. Marco, and R. Shah), Editzioi ETS, Pisa, vol. 1, 1999, pp 687-694.
[24] Nadler, M., and Mewes, D.: Effect of liquid viscosity on the phase distribution in horizontal gas–liquid slug flow, International Journal of Multiphase Flow 21, 1995b, 253–266.
[25] Nicklin, D.J., Wilkes, J.O. and Davidson, J.F.: Two-phase flow in vertical tubes, Trans. Inst. Chem. Engrs. 40, 1962, 61-68.
[26] Nydal, O.J.: An experimental investigation of slug flow, PhD Thesis, University of Oslo, 1991.

[27] Orell A.: Experimental validation of a simple model for gas-liquid slug flow in horizontal pipes, Chemical Engineering Science, Volume 60, Issue 5, 2004, pages 1371-1381.
[28] Ruzicka M.C., Drahos J., Fialova M.: Thomas N.H., Effect of bubble column dimensions on flow regime transition, Chemical Engineering Science, 56, 2001, 6117-6124.

[29] Sam R.G. and Crowley C.J.: Investigation of two-phase flow processes in coal slurry/hydrogen heaters, Final report DOE/PC 800028-T1, Creare Inc., Hanover, NH, 1986.
[30] Saxena S.C., Rao N.S., Saxena A.C.: Heat transfer and gas holdup studies in a bubble column: air-water-glass bead system, Chem. Eng. Commun, 96:1990, 31-55.
[31] Sekoguchi, K., Mori, K.: New development of experimental study on interfacial structure in gas–liquid two-phase flow, Exp. Heat Transfer Fluid Mech. Thermodynamics 2, 1997, 1177–1188.
[32] Schmidt, Z.: Experimental Study of Two-Phase Slug flow in a Pipeline-Riser Pipe System, Ph.D. dissertation, University of Tulsa, 1977.
[33] Sylvester, N.D.: A Mechanistic Model for Two-Phase Vertical Slug Flow in Pipes, Journal of Energy Resources Technology, Vol. 109, 1987.
[34] Taitel, Y., Barnea D., and Dukler A. E.: Modelling Flow Pattern Transitions for Steady Upward Gas-Liquid Flow in Vertical Tubes, AIChE J, 26, 1980, 345-354.
[35] Van Hout, R., Barnea, D., and Shemer, L.: Translational velocities of elongated bubbles in continuous slug flow, International Journal of Multiphase Flow, 28, 2002, 1333–1350.
[36] Wallis, G.B.: One dimensional Two Phase Flow, McGraw-Hill Book Co., New York, 1969
[37] White, E.T. and Beardmore, P.H.: The velocity of rise of single cylindrical air bubbles through liquids contained in vertical tubes, Chem. Eng. Sci., 17, 1962, 351-361.